International Conference on. Quenching and Distortion Engineering 2018,
November 27-29, 2018, Nagoya, Japan (Manuscript) Arimotech Report: www.arimotech.com

A Simulation Study on Blade Curving due to Quenching in the Japanese Sword

Muneyoshi Iyota[1,a *], Toshikazu Yoshii[2,b] and Kyozo Arimoto[3,c]

[1]Osaka Institute of Technology, 5-16-1, Omiya, Asahi-ku, Osaka, Osaka, Japan

[2]CHUGAI RO Co., Ltd., 2-4, Chikkoshinmachi, Nishi-ku, Sakai, Osaka, Japan

[3]Arimotech Ltd., 4-3-2, Habucho, Kishiwada, Osaka, Japan

[a]muneyoshi.iyota@oit.ac.jp,
[b]Toshikazu_Yoshii@n.chugai.co.jp,
[c]kyozo_arimoto@arimotech.com

Keywords: Japanese sword, Model Japanese sword, Quenching, Blade Curving, Simulation

Abstract. Experimental study on blade curving due to quenching in the Japanese sword was performed by our authors using prepared Japanese sword (JS)-type specimens made of the same steel and by the same process as the Japanese sword, and model JS-type specimens with almost the same shape as JS-type specimens, which were machined from commercial carbon steel S55C and austenite stainless steel SUS304 bars. All specimens quenched by a swordsmith using a traditional way showed a usual curved shape with different curvatures. In this study, changes of curving, temperature, microstructure, stress, and various kinds of strain were obtained by applying heat treatment simulation to this experiment, and a part of the results was confirmed to agree with the generated phenomenon. Examining distributions of various strains in a cross section of the specimens revealed that the curving in the model JS specimen made of SUS 304 (MJS-SUS304 specimen) is induced by positive plastic strain occurring near the cutting edge due to uneven cooling. On the other hand, the same examination clarified that curving of the model JS specimen made of S55C (MJS-S55C specimen) and the JS specimen was produced by not only similar plastic strain to in the MJS-SUS304 specimen but also expansion strain due to martensite transformation.

Introduction

It has long been known to swordsmiths that curving of the Japanese sword occurs during quenching. When knowledge about martensite and its density was obtained as a result of the development of steel engineering, it was explained that this curving is caused by lower density martensite occurring near the edge. On the other hand, Hattori [1] reported the two factor theory in 1929 based on the results of the one-sided quenching experiment using round steel bars, that is, the curving occurs with not only low density of martensite but also the plastic strain caused by unequal cooling.

As an educational topic for heat treatment distortion, Japanese heat treatment engineers have taken up the curving of Japanese sword. In general, the martensite theory is used more than the two factor theory for the explanation. In addition, it may be heard as a tentative theory that Japanese swords made of austenitic stainless steels do not curve because martensitic transformation due to quenching is not induced there.

The authors [2] performed quenching experiments using specimens having a shape similar to a real Japanese sword rather than a round bar for explaining the essence of the curving phenomenon in a way convinced by everyone. The Japanese sword (JS) type specimens made of the same steel as the Japanese sword was produced by a swordsmith. The cross-sectional shape of this specimen is the same as one of a traditional Japanese sword, however it is a uniform straight bar without a tip. Meanwhile, the authors made model JS type specimens with almost the same shape as the JS specimen by machining from bars of carbon steel (S55C) and austenitic stainless steel (SUS304). All specimens quenched in a traditional way by the swordsmith showed the normal curving of the Japanese sword with different curvatures.

In this study, heat treatment simulation was applied to this experiment and tried to explain the mechanism of curving generation. By appropriately setting the finite element model for each specimen, tendencies of simulated carvings became consistent with actual results. Furthermore, the reason for the curving generation was clarified by analyzing distributions of simulated various strains in the cross section of the specimens.

In the following sections, after outlining heat treatment simulation and an approach using simulated-strains, experimental and simulation conditions are described. Subsequently, the mechanism of curving generation in each specimen is expressed by analyzing distributions of various strains, after confirming agreement between experimental and simulated results.

Heat Treatment Simulation and Stress-Strain

Finite element simulation developed for studying heat treatment distortion has become available as commercial software, which can predict microstructure, temperature, distortion, stress, strain etc. occurring in parts during heat treatment processes. DEFORM^{TM}-HT [3] was used for simulation works in this study.

Using distributions of simulated strains, a procedure to explain the origin of distortion and stress generations was devised, which is called as the simulated-strain based approach [4]. This uses the relation on total strain ${}^t\varepsilon_{ij}$ and various strains obtained from simulation at time t:

$$ {}^t\varepsilon_{ij} = {}^t\varepsilon_{ij}{}^E + {}^t\varepsilon_{ij}{}^{TH} + {}^t\varepsilon_{ij}{}^{TR} + {}^t\varepsilon_{ij}{}^P + {}^t\varepsilon_{ij}{}^{TP} \quad (1) $$

where ${}^t\varepsilon_{ij}{}^E$, ${}^t\varepsilon_{ij}{}^{TH}$, ${}^t\varepsilon_{ij}{}^{TR}$, ${}^t\varepsilon_{ij}{}^P$ and ${}^t\varepsilon_{ij}{}^{TP}$ are elastic, thermal, phase transformation, plastic, and transformation plastic strains, respectively [4]. The strains in the right-hand side of Eq. (1), except the elastic strain, are obtained by adding their momentary occurrences from the initial state to the time t. In this study, a sum of the thermal and phase transformation strains is used as the expansion strain.

Experimental Conditions

Since details of the experiment are shown in the reference [2], some specific points are described here. Two kinds of specimens were prepared to clarify effects of different steels as follows:

(1) Japanese sword (JS) type specimen made by the swordsmith using the same steel and manufacturing processes as the Japanese sword.

(2) Model Japanese sword (MJS) type specimens made of carbon steel (S55C) and austenitic stainless steel (SUS 304) with almost the same shape as the JS specimen, which were produced by machining and named as MJS-S55C and MJS-SUS 304 specimens.

Above specimens have a length of 280 mm and a height and a maximum width of 30 and 8 mm, respectively, in the cross section. The detailed shape and dimensions are given in the reference [2]. Three holes for thermocouple insertion were provided on one end face of the specimen.

Prior to quenching, clay was applied on the surface of the three kinds of specimens in the same traditional manner by the swordsmith. Their quenching was carried out in a way that the swordsmith immersed specimens into water in a transparent acrylic container after heating it in a fire bed. The curving phenomenon of the specimens during quenching was recorded with a video camera. From images of the JS specimen during quenching, a remarkable reverse curving phenomenon was observed at the initial stage of cooling. On the other hand, it was not easy to recognize a reverse curving visually in the MJS-S55C specimen.

Simulation Conditions

The commercial software DEFORM^{TM}-HT was applied to quenching processes using the specimens. The outline and dimensions of the simulation model of the specimens are shown in Fig. 1. The half model was set using the symmetry of the cross section in the specimen. In the finite element division

of the model, the number of mesh divisions in the longitudinal direction is set to 140. On the other hand, the situation of finite element division on the cross sections of the JS specimens is shown in Fig. 2. Although the cross-sectional shape of the model of the MJS specimens is somewhat different [2], they used the sectional model of the JS specimen for convenience.

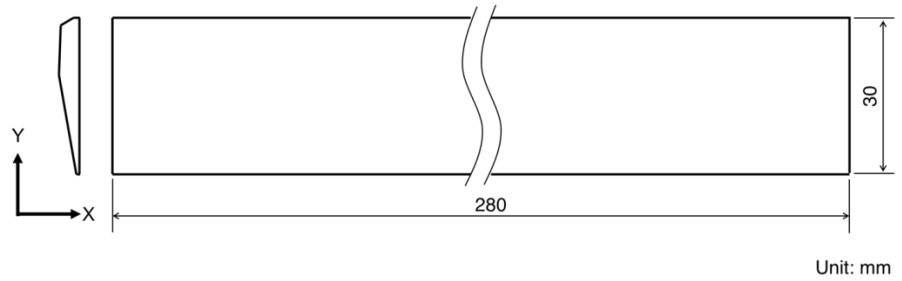

Fig. 1 Conceptual shape and dimension of simulation model.

In the simulation model, mechanical, thermal, and phase transformation properties were specified for the material. The mechanical and heat conduction properties for the MJS-SUS304 specimen were set by the data of the base material of SUS 304 included in the high temperature material property data collection on the dissimilar metal welding in reactor pressure vessel [5]. While, the properties of the carbon steel S55C for the MJS-S55C specimen model were provided by data collected at a series of research groups under the Japan Society for Heat Treatment. As for the Japanese sword steels used in the JS specimen, the amount of phosphorus and sulfur is smaller than those of commercially available steels as is widely known. The amount of carbon in regions of the specimen is adjusted by the swordsmith according to the purpose.

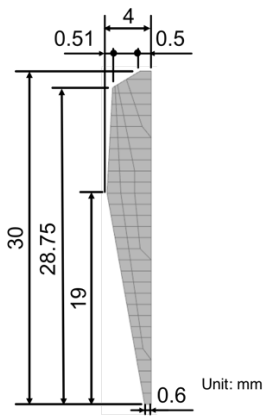

Fig.2 Section shape of simulation model.

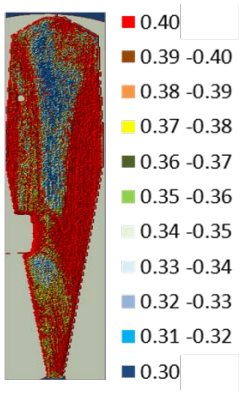

(a) EPMA measurement

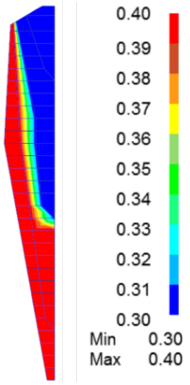

(b) Simulation condition

Fig. 3 Distribution of carbon concentration in JS specimen.

Japanese swords have been built by combining steels with different carbon concentration. Since the JS specimens were produced in the same way as Japanese swords, steel regions with different carbon concentrations are present inside. Fig. 3 (a) shows the measured carbon concentration distribution in the cross section of this specimen by Shimazu EPMA1610. Based on this measurement, the carbon concentration in the simulation model was specified as shown in Fig. 3 (b). Basically, the properties data of Japanese sword steels need to have carbon concentration dependency. The simulation software interpolates the data based on the carbon concentration distribution in Fig. 3 (b). Properties data of the Japanese sword steel was set in a form having carbon concentration dependency using carbon steel data collected by a series of research groups under the Japan Society for Heat Treatment.

Clay coating on the surfaces of specimens affects their heat transfer characteristics during cooling. The surface of the specimen models was divided into three regions based on the measurement data of

clay thickness as shown in Fig. 4. On the other hand, the simulation used three types of heat transfer coefficient of water corresponded to clay thickness as shown in Fig. 5. This data was obtained by applying the lumped heat capacity method to the cooling curves [6] measured at the center of a 10 mm diameter and 30 mm long silver cylinder probe coated with clay, and adjusting further to the results of this experimental study. Although the quenching was performed in a state of dispersion at the site, the condition of the simulation was specified as 800 °C in the heating temperature of the specimens and 20 °C in the temperature of the cooling water.

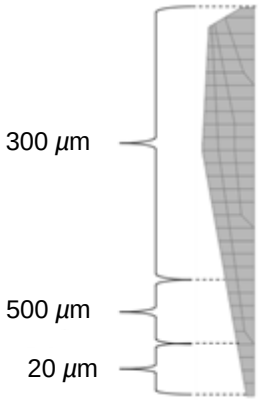

Fig. 4 Specified regions for different clay thickness.

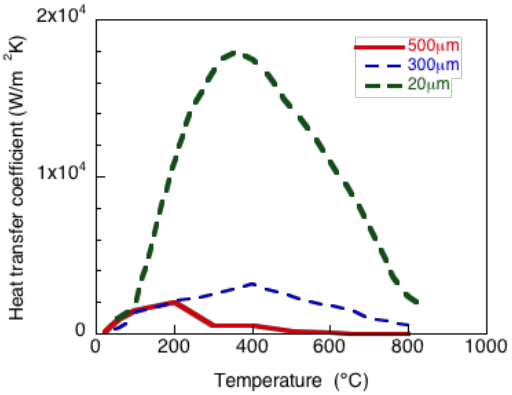

Fig. 5 Heat transfer coefficient for different thickness of clay.

Experimental and Simulated Results

Temporal changes of temperature and curving obtained from the experiment were compared with simulated results. First, cooling curves measured and simulated at three locations of the MJS-S55C specimen were shown in Fig. 6. The simulation used heat transfer coefficients of cooling as shown in Fig. 5. Both results agree sufficiently as shown in the figure. A similar degree of agreement was observed in the same comparison in the JS and MJS-SUS 304 specimens; however the results are omitted here because of space limitations.

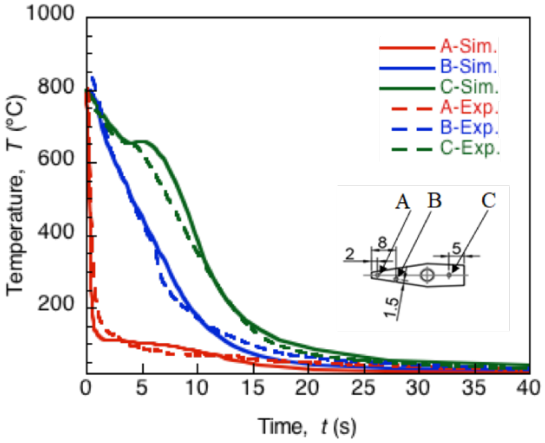

Fig. 6 Cooling curves obtained at points A, B, C.

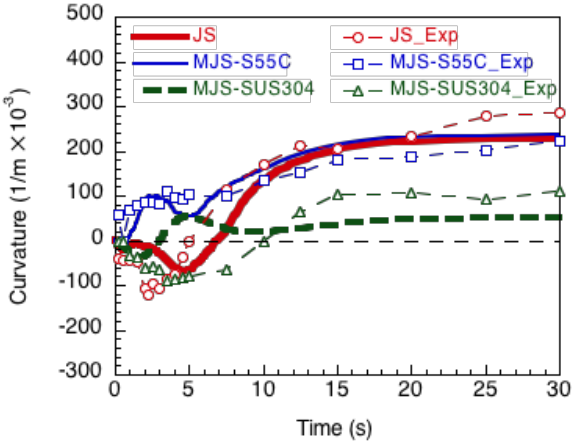

Fig. 7 Curvature changes of curving during cooling.

Changes of the curving curvature in specimens are shown Fig. 7 for comparing between measured and simulated results. It is defined a curvature of normal curving in the Japanese sword is positive. The measured values were obtained by examining video images at specific stages.

The MJS-SUS 304 specimen shows a negative curving curvature in the initial stage, which is called as a reverse curving, however it moves towards the positive direction as cooling progresses, and

finally it reaching to 100×10^{-3} m^{-1}. The simulation depicts an initial reverse curving, a positive curvature peak, and an attainment to the final value of 40×10^{-3} m^{-1} after decreasing the value.

The MJS-S55C specimen shows no reverse curving, while a positive curvature becomes eventually about 200×10^{-3} m^{-1} after increasing. The simulation predicts a larger variation than the MJS-SUS 304 specimen; thereafter it tends to be similar to the experiment. Finally, the experiment of the JS specimen depicts a reverse curving at the beginning, however as the cooling progresses, it goes in the positive direction and finally reaches about 300×10^{-3} m^{-1}. The simulation obtained the similar tendency in the curving although values do not agree well.

Curvature radii of the final curving in JS, MJS-S55C, and MJS-SUS 304 specimens were obtained as 3.0, 4.2, and 14.4 m, respectively, by measuring their shape.

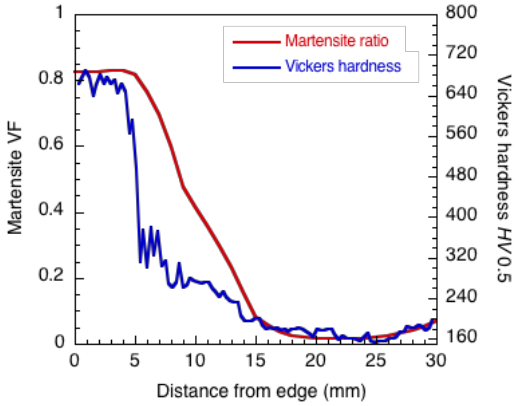

Fig. 8 Simulated martensite volume fraction and hardness in MJS-S55C specimen.

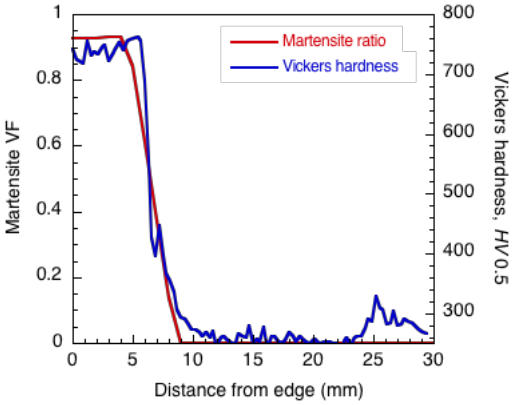

Fig. 9 Simulated martensite volume fraction and hardness in JS specimen.

The simulated volume fraction of martensite and measured hardness distribution along the axis of symmetry of the cross section in the JS and MJS-S55C specimens are plotted in Fig. 8 and 9, respectively. Vickers hardness distribution was measured at 300 μm intervals. There is a correspondence between volume fraction of martensite and hardness distributions.

Mechanism of Blade Curving

In order to explain the curving mechanism in the three types of specimens, changes in various strain distributions in the longitudinal direction in the cross section of the specimens are analyzed here based on the relationship of equation (1). Graphical representation of temperature, volume fraction of each phase, and longitudinal stress distributions is omitted because of space limitations.

MJS-SUS304 specimen

Temporal changes in the distribution of expansion, elastic, plastic, and total strains obtained from the simulation for the MJS-SUS 304 specimen are shown in Fig. 10. Time zero for the legend of the line corresponds to the state before quenching. Since there is no phase transformation in the SUS 304 steel, only thermal strain is included in expansion strain. As shown in Fig. 10 (a), this strain drops sharply near the cutting edge when quenching begins. On the other hand, positive plastic strain occurs and increases with time at the same place as shown in Fig. 10 (c), and reaches about 0.01 at the cutting edge. Finally it decreases to around 0.003.

Distributions of total strain are linear as shown in Fig. 10 (d), which means that a curved shape in a long object such as this specimen corresponds to a part of the arc. That is, a curving curvature can be obtained from a geometric relation from a distribution of total strain. Upward distribution at the initial stage corresponds to the reverse curving, and the subsequent downward one indicates the usual curved shape of the Japanese sword. Thermal strain is caused by changes in the temperature distribution. While, elastic strain shown in Fig. 10 (b) appears so as to satisfy the relation of equation

(1), and it becomes a negative value in the final state near the cutting edge. This corresponds to the generation of compressive stress. Initial reverse curving is due to the fact that expansion strain decreases near the cutting edge. On the other hand, the subsequent usual curved shape is contributed by positive plastic strain generated near the cutting edge.

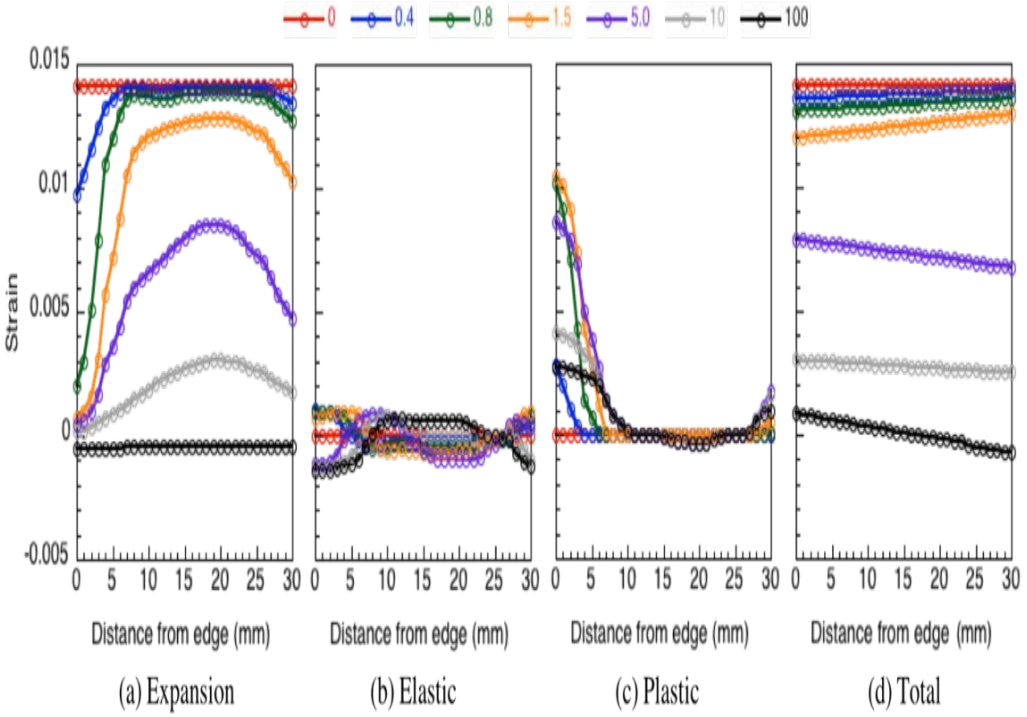

Fig. 10 Simulated Strains in MJS-SUS specimen section.

MJS-S55C specimen

Temporal changes of various strain distributions in the MJS-S55C specimen is shown in Fig. 11 in the same way as the previous figure. Since phase transformations occur in the S55C steel, generated transformation strain is included in the expansion strain shown in Fig. 11 (a). On the other hand, the transformation plastic strain shown in Fig. 11 (d) is generated by the effect of the phase transformation and stress generations. The transformation strain induces a positive swelling distribution of the expansion strain occurred near the edge in the final state of cooling. This is due to the contribution of martensite generated in this part. On the other hand, a negative transformation plastic strain occurs in the same region, however this is considered to be attributed to the state of stress when occurring martensite. As shown in Fig. 11 (c), a larger positive distribution of plastic strain remains as compared with the MJS-SUS 304 specimen.

As shown in Fig. 11 (e), distributions of total strain are almost horizontal in the initial stage of cooling. This corresponds to no occurrence of reverse curving as shown in Fig. 7. For example, at 0.8 s, it is considered that the total strain remains horizontal distribution because the decrease in the expansion strain is compensated by the increase in the transformation strain. The contribution of transformation plastic strain is small. At 1.5 s, the total strain is switched to the distribution of downward sloping due to the progress of plastic strain into the inside and the rise of the expansion strain on the surface side due to martensitic transformation.

At 10 s, the temperature is lowered as a whole, so that the expansion strain line becomes flat. As a result, the distribution of total strain shows a large downward slope due to a balance with other strains. Ultimately, its slope is larger than that of MJS-SUS 304. In the final distribution, the expansion strain is only the transformation strain due to martensite expansion near the cutting edge, and, in addition, the positive strain is the plastic strain near the cutting edge and the elastic strain in the inside. On the other hand, elastic strain and transformation plastic strain are negative at the edge and ridge sides. As these are added to the other strains, the downward slope of the total strain is increased. The obtained negative elastic strain corresponds to the compressive stress.

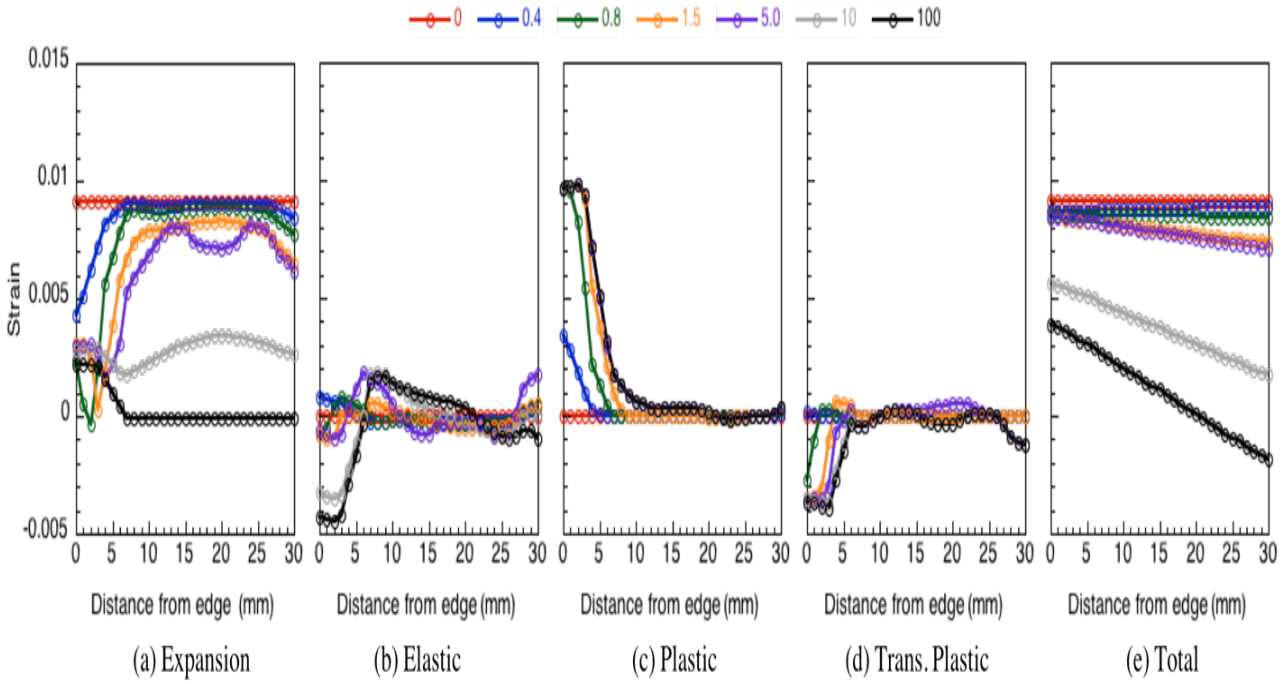

Fig. 11 Simulated Strains in MJS-S55C specimen section.

JS specimen

Figure 12 shows the temporal changes in the distribution of various strains in the JS specimen. These behave similarly to the MJS-S55C specimen, and finally almost the same total strain distribution occurs, which corresponds to the same level of curving. The reason for this occurrence is mainly contributions from the expansion strain due to the martensitic transformation in Fig. 12 (a) and the plastic strain in Fig. 12 (c). The elastic and transformation plastic strains shown in Fig. 12 (b) and (d), respectively, have some influence. In changes of the expansion strain shown in Fig. 12 (a), one at time zero is not a horizontal distribution. This is because the carbon concentration of the JS specimen is not uniform.

A notable difference in curving between the JS specimen and the MJS-S55C specimen appears as the different slope of the total strain at 5 s. Since the JS specimen has a distribution of carbon concentration, which may affect strain and stress generations in the cross section. Contributions to curving from such a point may be the future theme.

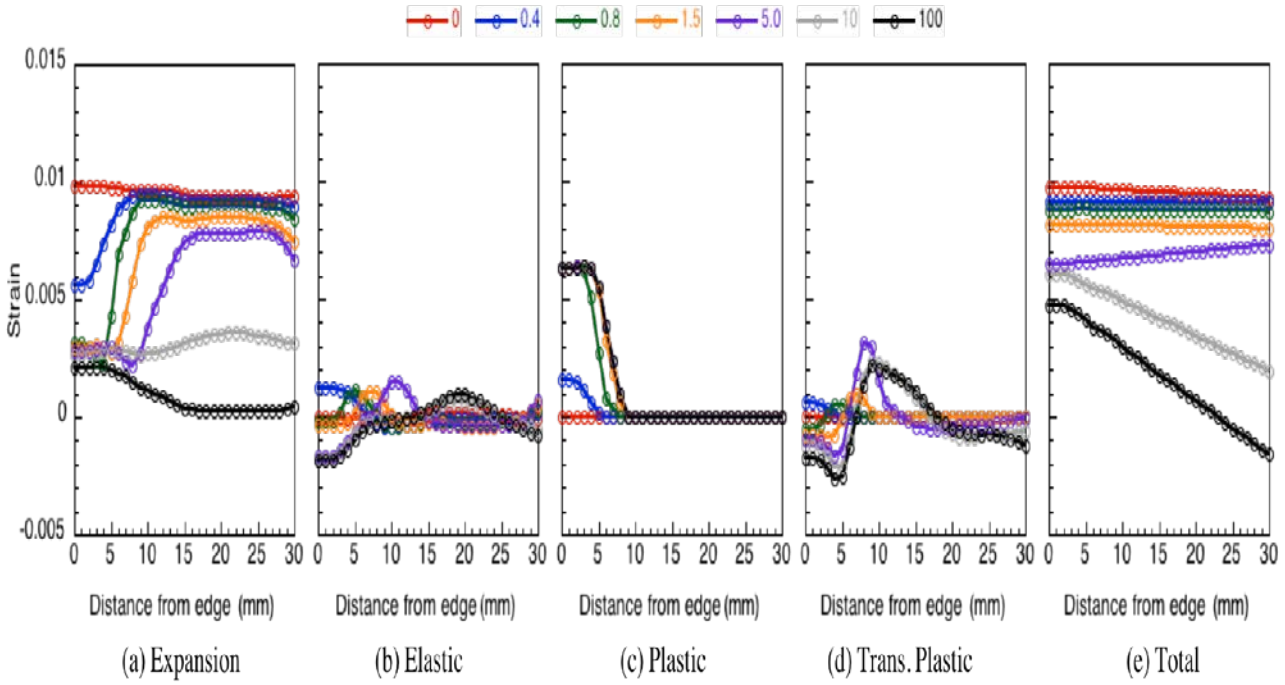

Fig. 12 Simulated Strains in JS specimen section.

Summary

In this research, the simulation was applied to quenching experiments using the JS specimen manufactured by the swordsmith and the model JS type specimen made of commercial steels. Based on the simulated results, the mechanism of curving generation was clarified by analyzing distributions of various longitudinal strains occurring in the cross section of the specimens. It was revealed that plastic strain in the MJS-SUS304 specimen and transformation and plastic strains in the MJS-S55C and JS specimens contribute mainly to the curving generation. From this, it became clear that the martensite theory for the Japanese sword curving, which had been proposed for a long time, is inadequate.

From the results of this quenching experiment and simulation, it is revealed that characteristics of specimens can be distinguished by conditions of curving and various strains. On the other hand, it is believed that this study is effective in evaluating data on material properties and heat transfer characteristics of cooling used in simulation. By newly developing a furnace, a specimen transfer device, in-situ curving measuring device, etc., it may be possible to realize a testing method for studying heat treatment distortion under various conditions.

In conducting this study, we received support from a number of key persons in specific fields including Mr. Sumihira Manabe, a swordsmith.

References

[1] D. Hattori, “On the Cause of Quenching Deformation in Tool Steels,” Science Reports of Tohoku University, Vol. 18, pp. 665–698, (1929)

[2] K. Arimoto and M. Iyota: “Study on Blade Curving Caused by Quenching of the Japanese Sword,” Materials Performance and Characterization (in press)

[3] K. Arimoto, G. Li, A. Arvind, and W. T. Wu: “The modeling of heat treating processes,” Proceedings of the 18th Heat Treating Conference, pp. 23-30 (1998)

[4] K. Arimoto: “Thermally-Processed Steels: Residual Stresses and Distortion,” In Encyclopedia of Iron, Steel, and Their Alloys, Taylor and Francis, New York, Published online: 13 Apr 2016; 3605-3633.

[5] Japan Nuclear Energy Safety Organization, “Project of Integrity Assessment of Flawed Components with Structural Discontinuity (IAF): Material Properties Data Book at High Temperature for dissimilar metal welding in Reactor Pressure Vessel”, JNES-RE-2012-24, (2013) (in Japanese)

[6] M. Narazaki, S. Fuchizawa, and N. Takeda: “Effect of surface coatings on cooling characteristics during water quenching of hot metals,” Netushori, Vol. 28 (5), 1988, pp. 279 – 285. (in Japanese)